



Effect of atmosphere change paths on the induced chemical expansion

Olivier Valentin, Eric Blond, Aurélie Julian, Nicolas Richet

► To cite this version:

Olivier Valentin, Eric Blond, Aurélie Julian, Nicolas Richet. Effect of atmosphere change paths on the induced chemical expansion. *Ceramics materials*, 2010, 62 (3), pp.283-287. hal-00604468

HAL Id: hal-00604468

<https://hal.science/hal-00604468>

Submitted on 29 Jun 2011

HAL is a multi-disciplinary open access archive for the deposit and dissemination of scientific research documents, whether they are published or not. The documents may come from teaching and research institutions in France or abroad, or from public or private research centers.

L'archive ouverte pluridisciplinaire **HAL**, est destinée au dépôt et à la diffusion de documents scientifiques de niveau recherche, publiés ou non, émanant des établissements d'enseignement et de recherche français ou étrangers, des laboratoires publics ou privés.

Effect of atmosphere change paths on the induced chemical expansion

Valentin O.^{1*}, Blond E.¹, Julian A.², Richet N.³

¹ Institut PRISME EA 4229, University of Orléans, Polytech'Orléans,
8 rue L. de Vinci, 45072 Orléans, France

² SPCTS - UMR 6638 - CNRS, 47 avenue Albert Thomas, 87065 Limoges, France

³ Air Liquide CRCD, 1 chemin Porte des Loges BP126, 78354 Jouy en Josas, France

Abstract

This study presents the relevant aspects of the approach developed at Institut PRISME to model strain in mixed ionic and electronic conductors (MIEC) membrane for reforming of methane into synthesis gas (H_2/CO). This macroscopic approach is based on the assumption of strain partition and on the choice of oxygen activity as state variable. It leads to a thermo-chemo-mechanical model taking into account the oxygen diffusion, the elastic, the thermal and the chemical expansions phenomena. A chemical expansion model is proposed. The kinetics of macroscopic bulk diffusion model has been fitted by simulation to chemical dilatometry tests. The transient and the steady-state stress distribution in a membrane reactor for partial oxidation of methane (POM) have been simulated in various conditions. The stress field depends on the atmosphere change history. The calculation shows that the stop in air is a critical loading case. The stop in N_2 induces relatively low stresses, but, the restarting from this last state is critical.

Introduction

Dense mixed ionic and electronic conducting membranes (MIEC) have potential applications for partial oxidation of methane (POM) into synthesis gases (CO/H_2) from the extraction of oxygen from air. The driving force of oxygen transport is ensured by the gradient of chemical oxygen potential. The diffusion of the oxygen ions induces changes of valence and oxygen vacancy variations which results in macroscopic strain [Atkinson2000, Miyoshi2003, Kharton2003]. The same phenomenon is observed in other applications of non-stoichiometric oxide such as Solid Oxide Fuel Cells (SOFC) [Yakabe2003, Fu2006]. In the POM process, the oxygen activity through the membrane may vary from oxidizing atmosphere (air) to reducing atmosphere (CH_4) in a range of more 20 orders of magnitude. In service, according to the boundaries conditions, it leads to strain-stress between oxidizing side and reducing side. At membrane reactor scale these chemo-mechanical stresses affect the mechanical reliability of the whole structure [Atkinson2000, Pei1995]. From our knowledge few authors like Yakabe [Yakabe2003] for SOFC, proposed a numerical simulation model to analyse in steady state the chemical and thermal expansion in interconnector.

This work focuses on the influence of the operating conditions on the membrane stress field. In the first part

the modelling of the chemical expansion is presented. The computational methods are then briefly described. In the next part, the identification method of kinetics is presented. The last part concerns various loading cases of simulations of a membrane.

Thermo-Chemo-Mechanical model

The chemical expansion is the strain which result of a change in composition of the material at constant phase. These changes can be caused by atmosphere and/or temperature variations. The chemically-induced strain does not modify the elastic mechanical behaviour but comes in addition to the usual thermal expansion [Adler2001].

Assuming small strains, the total strain tensor is described by the symmetric part of the displacement gradient with respect to the spatial position. Then, the partition of deformations leads to write the total strain as the sum of all possible strains:

$$\boldsymbol{\varepsilon} = \boldsymbol{\varepsilon}_t + \boldsymbol{\varepsilon}_e + \boldsymbol{\varepsilon}_c \quad (1)$$

Where $\boldsymbol{\varepsilon}_t$ is the thermal strain tensor, $\boldsymbol{\varepsilon}_e$ is the elastic strain tensor and $\boldsymbol{\varepsilon}_c$ the chemical strain tensor. In the rest of the paper, bold symbols will refer to vector/tensor variables and regular ones will refer to scalar parameters.

The thermal strain tensor depends on temperature variation in a reversible way:

$$\boldsymbol{\varepsilon}_t = \alpha(T - T_0)\mathbf{I} \quad (3)$$

Where α is the secant coefficient of linear thermal expansion, T_0 a reference temperature and \mathbf{I} the second rank identity tensor. The thermal deformation corresponds here exclusively to the deformation caused by temperature variation at constant composition and without any phase change.

Assuming the material is homogeneous and isotropic with linear thermal-elastic behaviour, the elastic strain is:

$$\boldsymbol{\varepsilon}_e = \frac{1+\nu}{E}\boldsymbol{\sigma} - \frac{\nu}{E}Tr(\boldsymbol{\sigma})\mathbf{I} \quad (2)$$

Where ν is the Poisson ratio, E the Young modulus, σ the stress tensor, \mathbf{I} the second rank identity tensor and $\text{Tr}(\sigma)$ is the trace of the tensor σ .

The coefficient of thermal expansion was measured by dilatometry ($\alpha_{20-900} = 1.1 \times 10^{-5} \text{ } ^\circ\text{C}^{-1}$). The Young modulus (125 GPa at 20°C, 95 GPa at 900°C) have been measured by the ultrasonic method [Julian2009a]. The tensile strength (120 MPa) and Weibull modulus (2.9) have been obtained using four point bending tests on a MTS-2/M testing machine with a load sensor of 10kN. Other data like Poisson ratio (0.25), thermal conductivity ($2 \text{ W.m}^{-1}.\text{ } ^\circ\text{C}^{-1}$) or specific heat ($500 \text{ J.Kg}^{-1}.\text{ } ^\circ\text{C}^{-1}$) have been chosen from literature values for such ceramics.

Chemical expansion model

The literature reports strains coming from variation of concentration of a substance in material [Krishnamurthy2004]. Theses strains are stress-free according to the approach of Larché *et al.* [Larché]. In order to model the thermo-chemo-mechanical behaviour of such ceramics, the majority of phenomenological works proposed a linear relation between the chemical expansion and the oxygen vacancy concentration [Hendriksen2000, Boroomand2000, Hilpert2003, Li2007]. However, Adler [Adler2001] considers only a dependence of the specific volume as a function of oxygen composition, temperature and pressure.

The chemical expansion model proposed hereafter is an improvement of previous studies [Blond2008, Valentin2009]. In theses models, it has been chosen to directly link chemical expansion to oxygen activity. The main assumption of the proposed approach is the reversible dependence of the chemical strain tensor with oxygen activity variation. Furthermore, because this work focuses on the atmosphere management effects, the temperature influence in relation to the chemical expansion is neglected. Therefore, at macroscopic scale, assuming isotropic chemical strain, three parameters are necessary to describe the dependence of chemical strain in relation to oxygen activity:

$$\begin{cases} \varepsilon_c = \beta \times \ln\left(\frac{a}{a_{ref}}\right) & \text{for } a \geq a_{min} \\ \varepsilon_c = \beta \times \ln\left(\frac{a_{min}}{a_{ref}}\right) = \varepsilon_c^{\max} & \text{for } a < a_{min} \end{cases} \quad (4)$$

Where ε_c is the linear chemical induced strain, β is a dimensionless coefficient of chemical expansion (-1.78×10^{-4}), a_{ref} is the zero chemical strain oxygen activity reference (air for our material), a is the actual oxygen activity at the considered point and a_{min} is the minimal oxygen activity under which the chemical expansion is constant (3×10^{-5}).

Fig. 1 shows the chemical expansion model fitted with both the results of dilatometry and X-ray measurements for $\text{La}_{0.8}\text{Sr}_{0.2}\text{Fe}_{0.7}\text{Ga}_{0.3}\text{O}_{3-\delta}$ perovskite-type material. This characterization of thermal and chemical expansion is fully detailed in [Valentin2009a]. $\text{La}_{1-x}\text{Sr}_x\text{Fe}_{1-y}\text{Ti}_y\text{O}_{3-\delta}$ material previously studied [Valentin2009] follows a similar behaviour and could be describe with the same model.

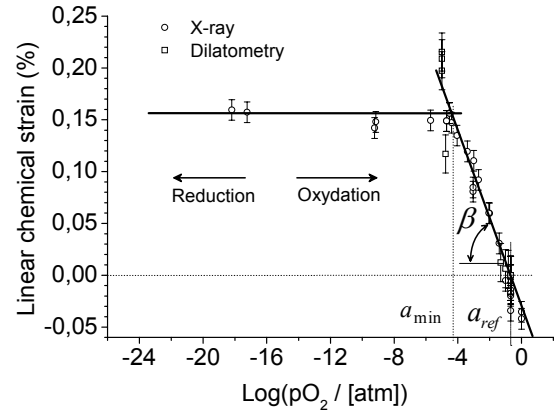


Fig. 1 Chemical expansion vs. oxygen activity, results by X-ray and dilatometry for $\text{La}_{0.8}\text{Sr}_{0.2}\text{Fe}_{0.7}\text{Ga}_{0.3}\text{O}_{3-\delta}$

The logarithmic matches the experimental results in a range of oxygen partial pressure from $p\text{O}_2 = 3 \times 10^{-5} \text{ atm}$ to $p\text{O}_2 = 1 \text{ atm}$. From $3 \times 10^{-5} \text{ atm}$ to 10^{-21} atm the chemical expansion appears constant.

Oxygen transport model

The oxygen diffusion can be represented using the simplified Wagner's law:

$$\mathbf{J} = D_0 e^{-Q/RT} \text{grad}(\ln a) \quad (5)$$

Where J is the oxygen flux, a the oxygen activity, D_0 the "intrinsic" oxygen diffusivity, Q the activation energy and R the ideal gas constant.

The time scale of permeation gets longer as the temperature is reduced. At low temperature ($< 500^\circ\text{C}$), the diffusion process is stopped because of the Arrhenius term in Eq. (5). Consequently, oxygen activity in material does not evolve and neither does chemical expansion. The surface exchanges are not considered in this study. This is still work in progress and would be presented in future papers.

Computational method

The chemical strain behaviour proposed above has been implemented in Abaqus finite elements software using the UMAT procedure. For the oxygen transfer computation a macroscopic modelling of oxygen permeation through the membrane according to the Eq. (5) has been implemented in UMAT procedure. The geometries of the cylindrical sample and tubular membrane have been modelled in 2D with axisymmetric elements. The oxygen activity is directly

applied on the boundaries. Computations are realized in three steps: heat transfer computation to obtain the temperature field; Oxygen transfer computation, using the temperature field to obtain the oxygen activity field; Thermo-mechanical simulation, including the dedicated strain behaviour, the temperature gradient and the oxygen activity distribution. Stringent numerical tests were performed to ensure that the solutions were independent of the mesh size.

Identification of the permeation kinetics

To identify the parameters of Eq. (5), the simulation of expansion test on cylindrical sample (6.7 mm diameter and 5 mm long) under N_2 and Air have been computed. The kinetics of heat transfers is assumed so much faster that oxygen permeation is the limiting step. Therefore, since the chemical expansion behaviour is known, the rate at which the sample exhibits its chemically-induced expansion expresses the kinetic of permeation. When the permeation starts (depending on the temperature) the chemical expansion occurs and a chemical strain adds to thermal strain on the expansion curves.

The prescribed conditions for the simulation of expansion tests are detailed in Fig. 2. The boundary conditions of oxygen activity are applied along the contour of the geometry: 10^{-5} for reducing and 0.21 for oxidizing. The homogenous temperature field is imposed at a constant heating and cooling rate of $2^\circ\text{C}/\text{mn}$. Classical mechanical boundary conditions are used to prevent rigid body displacements.

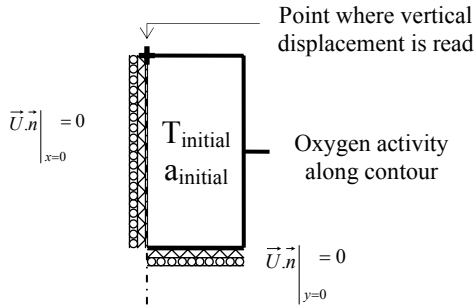


Fig. 2 Prescribed field and boundary conditions for the expansion test simulation

The material is in equilibrium with air (initial state air) at the beginning of the reduction test, whereas the material is in equilibrium with nitrogen for the oxidizing one (initial state N_2). More details about the dilatometry test are given in [Valentin2009]. Fig 3 for reducing and Fig. 4 for oxidizing step show how the simulations match experiments with $D_0 = 100 \text{ m}^2 \cdot \text{s}^{-1}$ and $Q = 138 \text{ kJ}$.

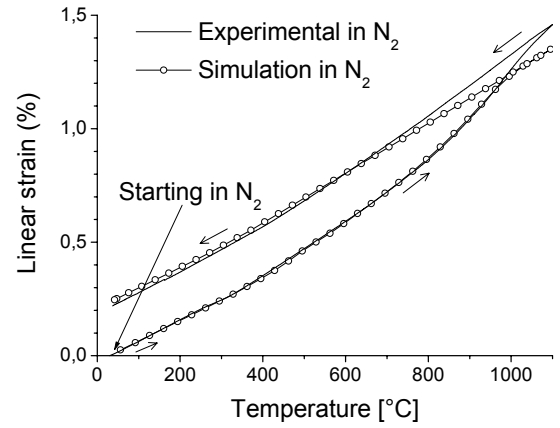


Fig. 3 Dilatometric curves in reducing, experimental vs. simulation, initial state is Air

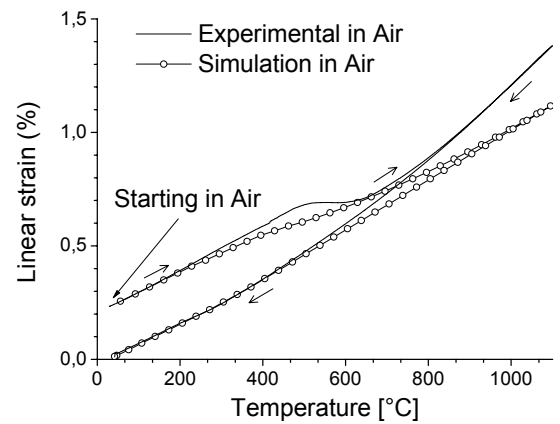


Fig. 4 Dilatometric curves in oxidizing, experimental vs. simulation, initial state is N_2

For the oxidizing test the deviation above 500°C should be attributed to the thermal sensitivity of chemical expansion as suggested in the companion paper on characterization [Valentin2009a].

It is significant to notice that the kinetic parameters are refined on the whole two tests, without distinction of oxidizing and reduction stage. The simulation stays in agreement with the experiment but the results suggest that the thermal activation of permeation differs between oxidizing and reduction. The oxidizing kinetics should be faster than reducing.

However, the shape of the chemical expansion behaviour (logarithm) as demonstrated in [Valentin2009] biases the perception of permeation kinetics when considering the dilatometry curves. Furthermore, the kinetics of diffusion represents probably one of the most complex aspects in MIEC. Adler [Adler2007] said that a consensus has not yet emerged regarding the mechanisms and rate laws governing exchange of oxygen with the bulk at the gas-exposed surface. It is necessary to refine more the kinetics to describe correctly the tests. The works are still in progress on a specific oxygen surface exchange law.

Simulations of a membrane

The thermo-chemo-mechanical simulations have been realized on a tubular membrane section of 7.2 mm inside diameter, 1 mm thickness. More information about the geometry of the reactor is presented in [Blond2008]. The prescribed conditions for the membrane simulation are detailed in Fig. 5. The constant and homogenous temperature field is fixed at 900°C in the structure.

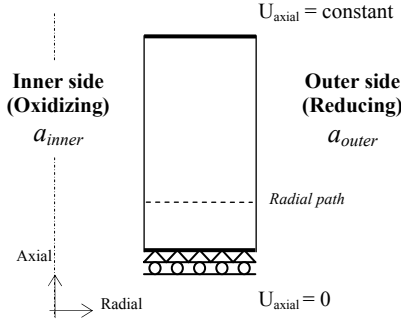


Fig. 5 Prescribed field and boundary conditions for the simulation of the tubular membrane section

In this study of atmosphere change path effect, the reference steady-state conditions chosen are a_{ref} on inner side and a_{min} on outer. In fact, it corresponds to air and N_2 respectively for the characterized material here. The transient states for various initial (N_2 or air) and final oxygen partial pressure (N_2 or air) are studied.

All the results of stresses distributions presented hereafter are plotted following the radial path in section of membrane (Fig. 5). The stress distributions have been normalized to unity with respect to the maximum tensile stress reached during the reference steady-state conditions (axial stress on inner side).

When reaching the reference steady-state, the oxygen activity gradient through the thickness gives rise to chemical stresses. The steady-state stress distribution is plotted in Fig. 6. It corresponds exactly to the typical case of a cylinder heated on outer side. If the atmosphere is reducing, the strain is positive and the stress is in compression. Vice versa, if the atmosphere is oxidizing, the strain is negative and the stress is in tension.

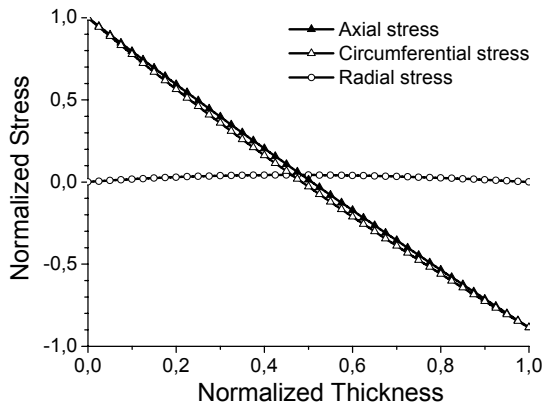


Fig. 6 Stresses due to chemical strain in membrane in steady-state

In the reference steady-state, axial and circumferential stresses are almost the same. The inside surface of the membrane is in tension and the outside in compression. In ceramic material the tensile stresses are dangerous especially when they occur on surface. The level of tensile stress is 109 Mpa which is in the range of tensile strength with a weibull modulus of 2.9. Therefore, the inner side is mechanically critical in this situation. The radial stress is negligible.

When harder conditions are applied on the reducing side ($< a_{min}$), the stress distribution in membrane is different because the chemical expansion under a_{min} is constant. This is plotted in Fig. 7. In steady state, the level of tensile stress on oxidizing side is 1.55 time higher than the level reached in the reference steady state. In highly reducing atmosphere, even if the chemical expansion is constant above a_{min} , it causes a worse situation for the mechanical reliability.

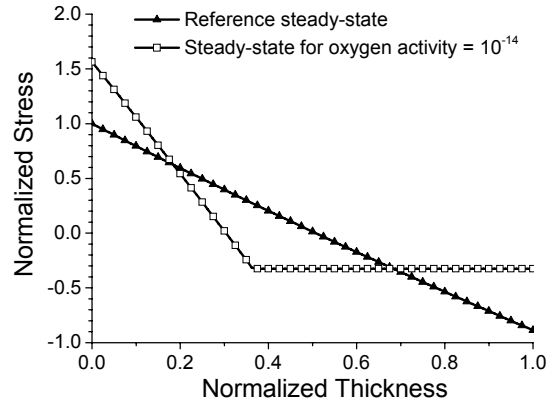


Fig. 7 Stress distribution due to chemical strain for oxygen activity reducing conditions under a_{min} (10^{-14})

Transient states

The transient states during the starts-up and the stops of oxygen permeation are studied. For the starts-up, the two computed cases only differ upon their initial state:

- Initial state air: oxygen activity equal to 0.21 in the whole membrane (e.g. material sintering in air)
- Initial state N_2 : oxygen activity equal to 10^{-6} in the whole membrane (e.g. material sintering in N_2)

The transient stresses due to chemical strain in membrane during start-up from initial state air to the reference steady-state are shown in Fig. 8.

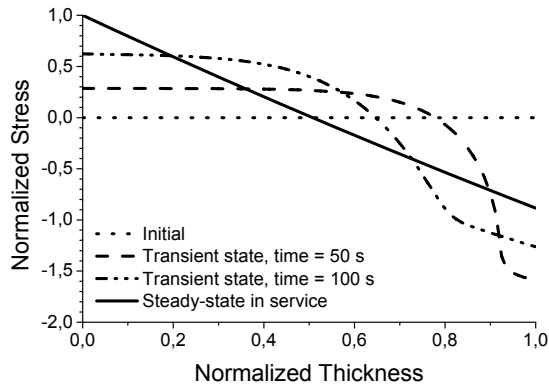


Fig. 8 Transient axial stresses due to chemical strain in membrane during start-up from initial state air to the reference steady-state

During start-up, there is tension of the inner side and compression of the outer side. The tensile stress on the inner surface increases from 0 to the stress of service. On the outer side the compressive stress reaches 1.6 times the compressive stress of steady state. Such as level are not especially damaging for ceramic material, because compressive strength is considered at less ten times as much as tensile.

The stress distributions during start-up from initial state N_2 to the reference steady-state are plotted in Fig. 8.

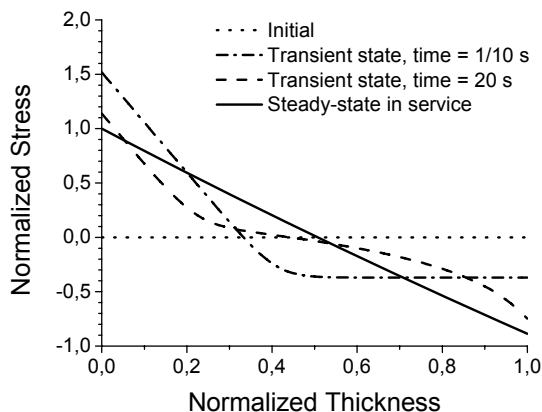


Fig. 9 Transient axial stresses due to chemical strain in membrane during start-up from initial state N_2 to the steady-state in service

This second case of start-up is critical because the tensile stress exceeds 1.5 times the tensile stress in

service. Consequently, this start-up is dangerous for the mechanical reliability of the membrane.

After reaching a permeation steady state in service, the atmosphere is switched in order to stop process. Two case stops are studied; they differ upon the condition prescribed on both the inner and outer sides.

First case, the oxygen activity on both the reducing and oxidizing surface is changed instantaneously from reference steady-state conditions to air. The stress distributions in the membrane during the next first time are presented Fig. 10 for this loading case.

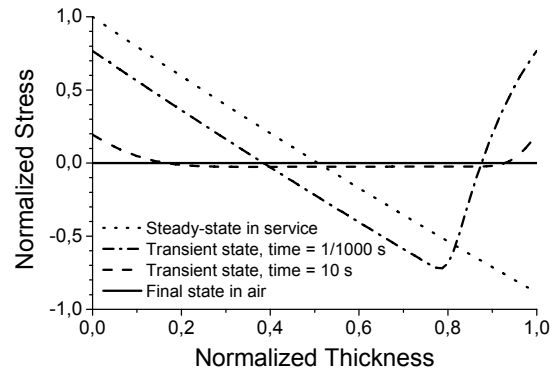


Fig. 10 Transient axial stresses due to chemical strain in membrane from the reference steady-state to final state air on the both sides

During the stop, the two faces are in tension (0.8 times as much as the stress in service) while the heart is in compression. This stress field is critical for mechanical reliability and thus should be avoided.

Second case, the oxygen activity on both the reducing and oxidizing surface is changed instantaneously from reference steady-state conditions to nitrogen. The transient stresses for the stop toward the final state N_2 are presented in Fig. 11.

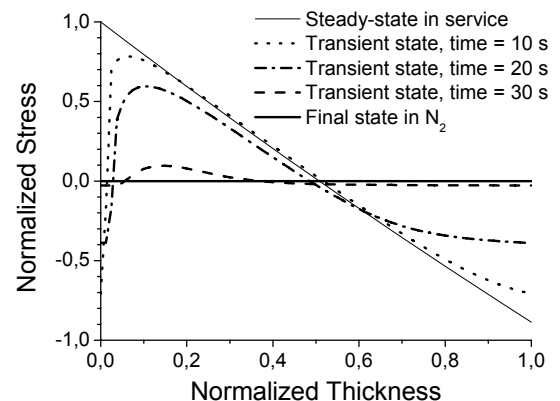


Fig. 11 Transient axial stresses due to chemical strain in membrane from the reference steady-state to final state N_2 on the both sides

This last stress field is not damaging for the membrane because the level of stress is continuously decreasing from the reference steady-state. The stop conditions in N_2 should thus be recommended. However after this,

the initial conditions for restarting the membrane will be the initial state in N_2 which is a particularly critical loading case as shown in Fig 9.

In order to avoid a restarting from initial state N_2 the membrane could be immersed in artificial air. This case is studied in Fig. 12.

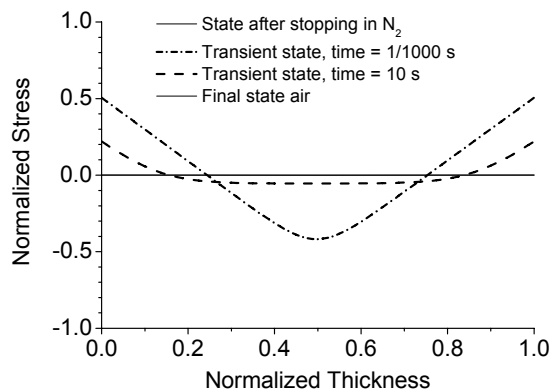


Fig. 12 Atmosphere treatment in Air to reach final state air

The stress level is 0.5 times lower than one of the reference steady-state, it is therefore reasonable to realize this atmosphere treatment before each restarting of reactor.

Conclusions

A thermo-chemo-mechanical has been proposed. It has been used to quantify mechanical stress in steady and transient state considering various atmosphere change path. This approach provides an indication of risks associated with the atmosphere changes. This numerical tool can help to develop a strategy to optimize the reactor lifetime.

The level of tensile stresses reached during steady-state is relatively high regarding the value of tensile strength and its weibull modulus. Moreover, the transient stages should be dangerous depending on the atmosphere change history. The calculation shows that the starting from initial state in equilibrium with air causes relatively low internal stresses. Conversely the stop by switch from reducing atmosphere to air is a critical loading case. Stopping under N_2 induces relatively low stresses but the restarting from this last state leads to critical stress.

Acknowledgements

The authors would like to express their gratitude to E. Véron, for X-ray measurement, F. Millot for advices and helpful discussions. The authors want to acknowledge Air Liquid and the ADEME for supporting this research.

References

- [1] Atkinson A. and Ramos T. M. G. M.: Chemically-induced stress in ceramic oxygen ion-conducting membranes, *Solid State Ionics*, 129 (2000) 259-269.
- [2] Miyoshi S., Hong J.-O., Yashiro K., Kaimai A., Nigara Y., Kawamura K., Kawada T. and Mizusaki J.: Lattice expansion upon reduction of perovskite-type $LaMnO_3$ with oxygen-deficit nonstoichiometry, *Solid State Ionics* 161 (3-4) (2003) 209-217.
- [3] Kharton V. V., Yaremchenko A. A., Patrakeeve M. V., Naumovich E. N. and Marques F. M. B.: Thermal and chemical induced expansion of $La_{0.3}Sr_{0.7}(Fe,Ga)O_{3-\delta}$ ceramics, *Journal of the European Ceramic Society* 23 (9) (2003) 1417-1426.
- [4] Yakabe H. and Yasuda I.: Model Analysis of the Expansion Behavior of $LaCrO_{3-\delta}$ Interconnector under Solid Oxide Fuel Cell Operation. *J. Electrochem. Soc.*, 150(1):A35-A45, 2003.
- [5] Fu Q.X., Tietz F., Lersch P. and Stover D.: Evaluation of Sr- and Mn-substituted $LaAlO_{3-\delta}$ as potential SOFC anode materials. *Solid State Ionics*, 177(11-12):1059-1069, April 2006.
- [6] Pei S. et al.: Failure mechanisms of ceramic membrane reactors in partial oxidation of methane to synthesis gas, *Catalysis Letters* 30 (1) (1995) 201-212.
- [7] Julian A., Juste E., Geffroy P.M., Tessier-Doyen N., Del Gallo P., Richet N., and Chartier T.: Thermal behaviour of $La_{0.8}Sr_{0.2}Fe_{1-x}Ga_xO_{3-\delta}$ ($x = 0$ or $x = 0.3$). *Journal of the European Ceramic Society*, In Press, Corrected Proof:–, 2009.
- [8] H. Yakabe and I. Yasuda. Model Analysis of the Expansion Behavior of $LaCrO_3$ Interconnector under Solid Oxide Fuel Cell Operation. *J. Electrochem. Soc.*, 150(1):A35-A45, 2003.
- [9] Adler S. B.: Chemical expansivity of electrochemical ceramics, *Journal of the American Ceramic Society* 84 (9) (2001) 2117-2119.
- [10] Krishnamurthy R. and Sheldon B. W.: Stresses due to oxygen potential gradients in non-stoichiometric oxides, *Acta Materialia* 52 (7) (2004) 1807-1822.
- [11] Larché F. C. and Cahn J. W.: Overview no. 41 the interactions of composition and stress in crystalline solids, *Acta Metallurgica* 33 (3) (1985) 331-357.
- [12] Hendriksen P. V., Larsen P. H., Mogensen M., Poulsen F. W., and Wiik K.: Prospects and problems of dense oxygen permeable membranes. *Catal. Today*, 56(1-3):283-295, February 2000.
- [13] Boroomand F., Wessel E., Bausinger H. and Hilpert K.: Correlation between defect chemistry and expansion during reduction of doped $LaCrO_3$ interconnects for SOFCs, *Solid State Ionics* 129 (1-4) (2000) 251-258
- [14] Hilpert K., Steinbrech R. W., Boroomand F., Wessel E., Meschke F., Zuev A., Teller O., Nickel H. and Singheiser L.: Defect formation and mechanical stability of perovskites based on $LaCrO_3$ for solid oxide fuel cells (SOFC), *Journal of the European Ceramic Society* 23 (16) (2003) 3009-3020.

- [15] Li Y., Maxey Evan R., Richardson Jr J. W., Ma B., Lee T.H. and Song S.-J.: Oxygen Non-Stoichiometry and Thermal-Chemical Expansion of $\text{Ce}_{0.8}\text{Y}_{0.2}\text{O}_{1.9-\delta}$ Electrolytes by Neutron Diffraction, *Journal of the American Ceramic Society* 90 (4) (2007) 1208–1214.
- [16] Blond E. and Richet N.: Thermomechanical modelisation of ion-conducting membrane for oxygen separation, *J. Eur. Ceram. Soc.*, (28) 793-801, 2008
- [17] Valentin O., Blond E., Julian A. and Richet N.: Loading path effect on the chemical expansion in substoichiometric LSF based Perovskite. *Computational material Sciences*, 2009
- [18] Valentin O., Blond E., Millot F., Julian A. Veron E., Ory S. and Richet N.: Thermal and Chemical expansion characterization of $\text{La}_{0.8}\text{Sr}_{0.2}\text{Fe}_{0.7}\text{Ga}_{0.3}\text{O}_{3-\delta}$, In 11th International Conference and Exhibition of the European Ceramic Society, 2009
- [19] Adler S.B., Chen X.Y. and Wilsona J.R.: Mechanisms and rate laws for oxygen exchange on mixed-conducting oxide surfaces. *Journal of Catalysis*, 245(1):91–109, January 2007.